Single and Dual Cation Sites in Zeolites: Theoretical Calculations and FTIR Spectroscopic Studies on CO Adsorption on K−FER

ARTICLE *in* THE JOURNAL OF PHYSICAL CHEMISTRY B · DECEMBER 2006

Impact Factor: 3.3 · DOI: 10.1021/jp0631331 · Source: PubMed

8 AUTHORS, INCLUDING:

Edoardo Garrone
Politecnico di Torino
286 PUBLICATIONS **7,259** CITATIONS
SEE PROFILE

Karel Frolich
University of Pardubice
16 PUBLICATIONS **212** CITATIONS
SEE PROFILE

Carlos Otero Areán
University of the Balearic Islands
224 PUBLICATIONS **5,240** CITATIONS
SEE PROFILE

Dana Nachtigallová
Academy of Sciences of the Czech Republic
71 PUBLICATIONS **1,826** CITATIONS
SEE PROFILE

Single and Dual Cation Sites in Zeolites: Theoretical Calculations and FTIR Spectroscopic Studies on CO Adsorption on K-FER

E. Garrone,[†] R. Bulánek,[‡] K. Frolich,[‡] C. Otero Areán,[§] M. Rodríguez Delgado,[§] G. Turnes Palomino,[§] D. Nachtigallová,[||] and P. Nachtigall*,[||]

Dipartimento di Scienza dei Materiali ed Ingegneria Chimica, Politecnico di Torino, I-10126 Turin, Italy, Department of Physical Chemistry, University of Pardubice, Nám. Cs. Legií 565, 53010 Pardubice, Czech Republic, Departamento de Química, Universidad de las Islas Baleares, E-07122 Palma de Mallorca, Spain, and Institute of Organic Chemistry and Biochemistry, Academy of Sciences of the Czech Republic and Center for Biomolecules and Complex Molecular Systems, Flemingovo n. 2, CZ-16610 Prague, Czech Republic

Received: May 22, 2006; In Final Form: September 4, 2006

Interaction of CO with K-FER zeolite was investigated by a combination of variable-temperature IR spectroscopy and computational study. Calculations were performed using ω_{CO}/r_{CO} correlation method in combination with a periodic density functional theory model. On the basis of agreement between experimental and calculated results, the following carbonyl complexes were identified: (i) mono- and dicarbonyl C-down complexes on single K^+ sites characterized by IR absorption bands at 2163 and 2161 cm^{-1}, respectively; (ii) complexes formed by CO bridging two K^+ ions separated by about 7−8 Å (dual sites) characterized by a band at 2148 cm^{-1}; and (iii) isocarbonyl (O-down) complexes characterized by a band at 2116 cm^{-1}. The bridged carbonyl complexes on dual K^+ sites are about 5 kJ/mol more stable than monodentate (monocarbonyl) CO complexes. The C−O stretching frequency of monocarbonyl species in K-FER depends on K^+ location in the zeolite, and not on K^+ coordination to the framework. A combination of theoretical calculations using a periodic density functional model and experimental results showed formation of two types of monocarbonyls. The most abundant type appears at 2163 cm^{-1}, and the less abundant one at 2172 cm^{-1}. These experimentally determined wavenumber values coincide, within ±2 cm^{-1}, with those derived from theoretical calculations.

1. Introduction

Reversible gas adsorption on zeolites is at the basis of several industrial processes involving gas separation (from gas mixtures) and purification, and atmosphere pollution control. In the case of alkali-metal-exchanged zeolites, adsorbed molecules interact mainly with extraframework (exchangeable) cations. Differences in strength of the corresponding interaction forces for different molecules facilitate selective adsorption and gas separation. While these general concepts constitute a common background in zeolite science and technology, many details are poorly understood, and yet knowledge about fine details holds the key to further advances in the above (and related) technological fields.

Regarding carbon monoxide, most studies about its adsorption on alkali-metal-exchanged zeolites have focused on the interaction of this molecule mainly through the carbon atom,[1−3] but also through the oxygen end,[3,4] with isolated (extraframework) metal ions. However, in recent years experimental evidence (mainly from IR spectroscopic studies) is accumulating to suggest that pairs of metal cations can also constitute CO adsorption centers.[5,6] Detailed analysis of such possible cationic dual sites constitutes the main aim of the present work. For such a purpose, we combined variable-temperature FTIR spectroscopic studies with theoretical calculations performed using a periodic density functional (DFT) model. K-FER was chosen (mainly) because it has a relatively small unit cell amenable to DFT studies which, different from small cluster models, give due consideration to the zeolite framework topology.[7]

In essence, the layout of this study is as follows. First, periodic DFT calculations are used to locate the different K^+ sites within the FER unit cell; different Si/Al ratios were considered. Second, CO coordination to these sites is analyzed, and the CO stretching frequencies of the adsorbed molecule and the corresponding interaction energies are calculated. Finally, the calculated results are compared with those obtained from variable-temperature FTIR spectroscopy, which yields experimental values on the C−O stretching frequency of (different) adsorbed CO species, and also (whenever possible) on the corresponding standard adsorption enthalpy.

2. Materials and Methods

2.1. Experimental Details. The ferrierite sample used in this study was obtained from Zeolyst International; it was in the ammonium form and had a nominal Si:Al ratio of 27.5:1. From the parent zeolite, the potassium-exchanged sample (having 100% exchange level) was obtained by repeated ion exchange with a 0.5 M aqueous solution of potassium nitrate. Powder X-ray diffraction of the exchanged sample showed good crystallinity, and all diffraction lines corresponded to the FER structure type. Complete ion exchange was checked by the absence of IR absorption bands corresponding to either the ammonium ion or the Brønsted acid Si(OH)Al group, which

* To whom correspondence should be addressed. Phone: +420-220-410-314. Fax: +420-220-410-320. E-mail: petr.nachtigall@uochb.cas.cz.
[†] Politecnico di Torino.
[‡] University of Pardubice.
[§] Universidad de las Islas Baleares.
[||] Academy of Sciences of the Czech Republic and Center for Biomolecules and Complex Molecular Systems.

10.1021/jp0631331 CCC: $33.50
Published on Web 10/18/2006

would be generated during thermal activation (see below) of the zeolite sample if total exchange of potassium for ammonium did not take place in the parent NH_4−FER. For comparison (see Section 4), a K-FER sample having a Si:Al ratio of 8.6:1 was also used. This sample was obtained (as above) from the corresponding ammonium form, supplied by Research Institute of Inorganic Chemistry, Ústí nad Labem.

For IR spectroscopic measurements, thin self-supported wafers of the zeolite samples were prepared and activated (outgassed) in a dynamic vacuum (residual pressure $< 10^{-4}$ Torr) for 3 h at 650 K inside an IR cell[8] which allowed in situ sample activation, gas dosage, and variable-temperature IR spectroscopy to be carried out. For better thermal contact between the zeolite wafer and the cooled environment, 0.1 Torr of helium was admitted into the sample compartment before recording the background spectrum at liquid-nitrogen temperature. The cell was then dosed with CO and closed, and IR spectra were recorded at fixed temperature values within the 170−230 K range, while simultaneously registering sample temperature and equilibrium pressure inside the cell. A platinum resistance thermometer (Tinsley) and a capacitance pressure gauge (MKS, Baratron) were used for this purpose. Pressure correction (for helium) was determined from a calibration plot, as described elsewhere.[9] Transmission FTIR spectra were recorded, at 3 cm^{-1} resolution, using a Bruker IFS66 spectrometer.

2.2. Models and Computational Methods. *2.2.1. Models.* Calculations were performed using a periodic model of the orthorhombic unit cell (UC) of ferrierite (*Immm* space group) containing 36 T atoms (Si or Al) and 72 O atoms. The equilibrium volume of the all-silica FER unit cell (cell parameters $a = 19.1468$ Å, $b = 14.3040$ Å, and $c = 7.5763$ Å, volume 2076.70 $Å^3$) fitted previously[10] was used for all calculations on CO/K^+-FER. Two situations were investigated as described below.

(i) Model of High-Silica FER. One framework Si atom was replaced by one Al atom, and one K^+ (charge compensating cation) was added; the Al atom was subsequently placed at each of the four distinguishable framework T-sites (T1 to T4 following Vaughan's numbering[11,12]), and all possible K^+ sites in the vicinity of framework AlO_4 tetrahedron were investigated. For K^+ sites, the nomenclature introduced originally for Cu-MFI,[13] and recently adopted also for FER,[14,15] is used. The sites in the main channel, in the perpendicular channel, and at channel intersections are denoted M, P, and I, respectively. This model corresponds to a high-silica FER of composition $KAlSi_{35}O_{72}$ and a Si/Al ratio of 35. Calculations for K^+ at M7/T3 site were performed with a double-UC (composition $KAlSi_{71}O_{144}$), since in this case CO is oriented along the *c*-axis, and due to the small dimension of FER UC along this direction the CO molecule interacts with K^+ and with its periodic image when a single-UC is used. The use of a double-UC for other K^+ sites does not affect the calculated frequencies and interaction energies.

(ii) Model of Al-Rich FER. Four framework Si atoms were replaced by four Al atoms and charge balanced by 4 K^+ ions; this model represents a FER sample with composition $K_4Al_4Si_{32}O_{72}$ and Si:Al = 8. Up to four CO molecules were adsorbed in a FER unit cell.

In addition to the periodic DFT model, cluster model calculations were also performed using a simple 1-T cluster and a double 2x(1-T) cluster, $Al(OH)_4K$−CO, and $Al(OH)_4K$−CO−$KAl(OH)_4$, respectively. C_{2v} symmetry constraints were applied in all calculations with cluster models.

TABLE 1: Parameters of the ω_{CO}/r_{CO} Correlation for CO/K^+-Zeolite Systems[a]

complex	method basis set[a]	a [$Å^{-1}$ cm^{-1}]	b [cm^{-1}]	$\Delta\omega$ [cm^{-1}]
C-down	PBE/400 eV	−5443.0	8400.5	−2.3
	PBE/BS1	−5876.0	8864.5	−3.9
O-down	PBE/400 eV	−6376.8	9455.1	−3.1
	PBE/BS1	−7295.1	10470.2	−1.2

[a] For details, see section 2.2.

2.2.2. Computational Methods. Periodic DFT calculations were performed using the Perdew−Burke−Ernzerhof (PBE) exchange-correlation functional[16,17] and the projector augmented wave approximation (PAW) of Blöchl, as adapted by Kresse and Joubert.[18,19] The plane wave basis set with a kinetic energy cutoff of 400 eV was used. Brillouin-zone sampling was restricted to the Γ-point. Calculations were performed using the VASP program.[20−23] Zero-point energy (ZPE) corrections were calculated within the harmonic approximation using 6 degrees of freedom (for every CO molecule in the model system) for $(CO)_n$−$KAlSi_{35}O_{72}$ ($n = 1, 2$) and CO−$K_4Al_4Si_{32}O_{72}$ periodic DFT models. ZPE was calculated for monocarbonyl (both, C-down and O-down adducts), dicarbonyl, and bridged CO complex for K^+ ion(s) in I2/T2 site, and this correction was used for all complexes of any given type. The sum of the electronic interaction energy and ZPE gives the internal energy change at 0 K, $\Delta U^0(0)$. Experimental determination of standard adsorption enthalpy, ΔH^0, was carried out at temperatures around 200 K; therefore, $\Delta H^0(200)$ was evaluated from the ideal gas model ($\Delta H^0(T) = \Delta U^0(0) + (^7/_2)RT$).

The CO stretching frequencies calculated at the DFT level are not expected to give results directly comparable with experimental spectra. Recently, a ω/r correlation method was introduced[24] that, by correlating the r(CO) bond lengths obtained at the DFT level with CO stretching frequencies calculated at the coupled cluster level, gives the CO stretching frequency with near spectroscopic accuracy for metal carbonyl species at various environments.[25] Aside from the fact that the ω/r correlation method gives much more reliable results than a standard methodology for calculating frequencies (DFT and harmonic approximation), the ω/r correlation method does not require construction of the Hessian matrix of the CO/M^+-zeolite system. Instead, only the r(CO) bond lengths need to be determined at the DFT level.

Let us consider the C-bonded complexes. Within the concept of ω/r correlation method, the CO stretching frequencies are calculated from the equation

$$\nu_{CO}\,[cm^{-1}] = a r_{CO}\,[Å] + b + \Delta\nu + \Delta\omega \qquad (1)$$

where a and b were obtained from CCSD(T) calculations on the set of testing molecules, K^+CO, $H_2O...K^+CO$, $(H_2O)_2...K^+$-CO, $F^-...K^+CO$, and $(F^-)_2...K^+CO$; a correlation consistent valence-quadruple-ζ basis set with polarization functions (cc-pVQZ) basis set[26,27] was used on all atoms except K, for which a CVQZ basis set[28] suitable for correlation of 3s and 3p electrons was used. A constant anharmonicity correction for C−O stretching, $\Delta\nu = -29$ cm^{-1}, was assumed.[25] A $\Delta\omega$ correction was obtained as the difference between C−O stretching frequency calculated from eq 1 and those explicitly calculated at the CCSD(T) level for the $Al(OH)_4K$−CO (1-T) model. The same type of correlation was also obtained for O-down adducts. The results are shown in Table 1. Details of the method can be found elsewhere.[29]

Calculations on cluster models were performed using PBE exchange-correlation functional and relativistic small core ECP[30]

TABLE 2: CO Vibration Frequencies, Electronic Interaction Energies, and Adsorption Enthalpies of Mono- and Dicarbonyl Complexes on Single K^+ Sites in FER

Al position[a]	K^+ site[b]	CO complex[c]	location[d]	r(KC)[e] r(KO)[e]	r(CO)[f]	ν(CO)[g]	ΔE^{el}[h]	$\Delta H^0(200)$[h]
T1	P8	CO	P	3.062	1.1387	2171	−14.9	−18.1
11%		2 × CO	P	3.058	1.1387	2171		
			P	3.222	1.1409	2160	−5.1	−8.4
		OC	P	2.927	1.1473	2107	−9.6	−13.9
T2	I2	CO	P	3.133	1.1398	2165	−17.1	−20.3
22%		2 × CO	P	3.118	1.1401	2164		
			M	3.167	1.1402	2163	−15.5	−18.8
		OC	P	2.975	1.1459	2116	−10.9	−15.2
T3	M7[i]	CO	M	3.189	1.1401	2164	−15.6	−18.7
22%		2 × CO	M	3.206	1.1405	2162		
			M	3.150	1.1406	2161	−15.0	−18.3
		OC	M	3.053	1.1460	2115	−9.1	−13.5
T4	I2	CO	M	3.152	1.1399	2165	−17.2	−20.4
45%		2 × CO	M	3.195	1.1402	2163		
			P	3.183	1.1399	2165	−15.7	−19.0
		OC	M	3.003	1.1458	2117	−11.7	−16.1

[a] Percentual population of T-site in the framework is also given. [b] For site notation see Figure 1. [c] Monocarbonyl, dicarbonyl, and isocarbonyl complexes reported. [d] P and M stands for CO located in P cage and in M channel, respectively. [e] Distance (in Å) between K^+ and C or O atom of CO for C-down and O-down complexes, respectively. [f] In Å. [g] In cm^{-1}. [h] In kJ/mol. [i] Calculated with doubled UC.

TABLE 3: Complex Geometry, C−O Vibration Frequency, Electronic Interaction Energy, and Adsorption Enthalpy of Bridged Carbonyl Complexes on Dual K^+ Sites in FER[a]

K^+ site		CO location[c]	r(K−K)	r(K−C)	r(K−O)	r(CO)	ν(CO)[b] C-on	ν(CO)[b] O-on	ΔE^{el}	$\Delta H^0(200)$
M7/T3	M7/T3	M∥	7.58	3.227	3.749	1.1414	2157	2145	−17.9	−20.9
I2/T4	I2/T4	M⊥	7.21	3.132	3.027	1.1414	2157	2145	−22.1	−25.1
I2/T4	I2/T4	P	7.28	3.159	3.042	1.1419	2154	2141	−19.4	−22.4
I2/T2	I2/T2	M⊥	7.41	3.198	3.066	1.1420	2154	2141	−20.2	−23.2
I2/T2	I2/T2	P	7.15	3.121	2.975	1.1415	2156	2144	−20.9	−23.9

[a] Bond lengths and energies in Å and kJ/mol, respectively. [b] CO frequency (in cm^{-1}) calculated using ω_{CO}/r_{CO} correlation for C-on and O-on complexes. [c] M∥ and M⊥ stand for CO located along and across M channels, respectively, and P denotes CO in P cage.

augmented with two sets of d functions,[31] valence triple-ζ-plus-polarization function basis set for C and O atoms, and valence double-ζ-plus-polarization function basis set[32] for the other atoms (this combination of basis sets is denoted BS1). Interaction energies were corrected for the basis set superposition error (BSSE).[33] Calculations with atom-centered basis set were carried out with the Gaussian03 program suite.[34]

3. Results

3.1. Calculations. The nomenclature used for the K^+ sites and for the CO adsorption complexes is as follows. K^+ ion sites not having nearby cations are termed "isolated sites", while pairs of K^+ ion sites (at a distance of about 7−8 Å) are termed "dual sites". For CO adsorption complexes, the term "monocarbonyl" is used for CO interacting with only a single K^+ ion, via either the carbon or the oxygen atom (carbonyl and isocarbonyl complexes, respectively); "dicarbonyl" species are formed when two CO molecules interact with the same K^+ ion. The term "bridged CO complex" is used for CO interacting with the two K^+ ions of a dual site. Calculated characteristics for carbonyl complexes on isolated and dual sites are summarized in Tables 2 and 3, respectively.

3.1.1. K^+ sites in FER. The most stable K^+ sites in the vicinity of Al in T1, T2, T3, and T4 are depicted in Figure 1. When the framework Al atom is in T2 or T4 position, which are located on the eight-member ring entrance window of the perpendicular channel, the K^+ cation preferentially binds close to the center of this eight-member ring (Figure 1b,d). These sites, denoted I2/T2 and I2/T4, are located on the intersection of main (M) and perpendicular (P) channels. For Al atom in T3 position, the K^+ ion is located on top of the six-member ring on the wall of the main channel (denoted M7/T3, Figure 1c), and for Al atom in T1 position the K^+ ion preferentially binds on top of the eight-member ring window on the wall of perpendicular channel cavity (P8/T1 site, Figure 1a). In the case of Al atom in T1 or T2 framework positions, the P8/T1 and I2/T2 sites are the only sites that can have a significant population since the other K^+ sites are over 28 kJ/mol above the most stable site. On the contrary, P8/T3 and P8/T4 sites are only about 7 kJ/mol above the corresponding minimum energy sites, M7/T3 and I2/T4, respectively. Only the results for the most stable K^+ sites in the vicinity of each of the distinguishable framework T-site are reported in Table 2. More details about alkali-metal sites in FER will be described elsewhere.

3.1.2. CO Interaction with Isolated K^+ Sites in FER. The strongest interaction of CO with K-FER was found for two intersection sites (I2/T2 and I2/T4) where the electronic interaction energy ΔE^{el} is about −17 kJ/ mol. In both cases, the CO molecule is aligned along the P-channel direction. For both K^+ intersection sites, there are two stable complexes, facing the P channel cavity and crossing the M channel (P and M complexes, respectively) that have rather similar interaction energy and vibrational frequency. Only the most stable complexes for each of the intersection sites are reported in Table 2. The CO adsorption complexes on intersection I2 site show C−O vibrational frequency at 2165 cm^{-1}. The CO adsorption complexes on K^+ at M7/T3 site show $\Delta E^{el} = -15.6$ kJ/mol (about 1.5 kJ/mol above the complexes at I2 sites) and $\nu_{CO} = 2164$ cm^{-1}. The least stable CO adsorption complex was found for K^+ in P8/T1 site, where $\Delta E^{el} = -14.9$ kJ/mol and $\nu_{CO} = 2171$ cm^{-1}.

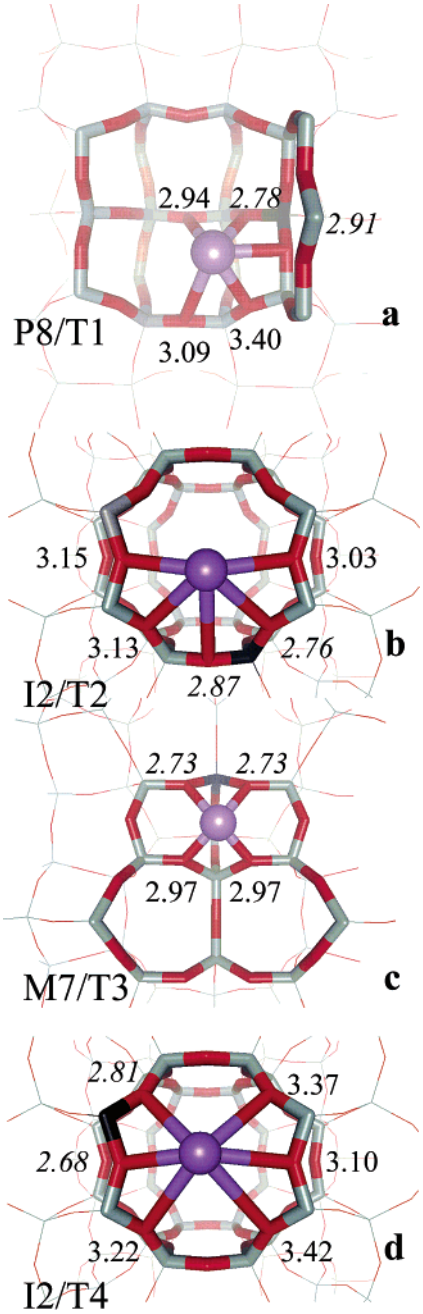

Figure 1. Most stable K^+ sites in FER for each of four distinguishable framework Al positions: (a) P8/T1 site in the FER P-cage, (b) I2/T2 site at the eight-member ring entrance window at the intersection of M and P channels, (c) M7/T3 site on the wall of the main channel, and (d) I2/T4 site at the eight-member ring entrance window. Framework O, Si, and Al atoms are depicted in red, gray, and black, respectively, and the K^+ cation is depicted as violet ball. The distances (in Å) between K^+ and framework oxygen atoms are also reported; italic is used for oxygen atoms of AlO_4 tetrahedra.

The intersection I2/T2 and I2/T4 sites can readily form dicarbonyl species with one CO molecule facing the P channel cavity and the other CO molecule directed across the M channel (Figure 2a). For K^+ in M7/T3 site the dicarbonyl species can also be formed with both CO molecules oriented along the main channel but in opposite direction (Figure 2b). In all of these cases the interaction energy of the second CO molecule is close to that of the first molecule ($\Delta E^{el} = -15.0$ kJ/mol). Also, the CO stretching frequencies are rather similar for mono- and dicarbonyl species; ν_{CO} is at the most 3 cm^{-1} lower for dicarbonyl than for monocarbonyl complexes. The only stable

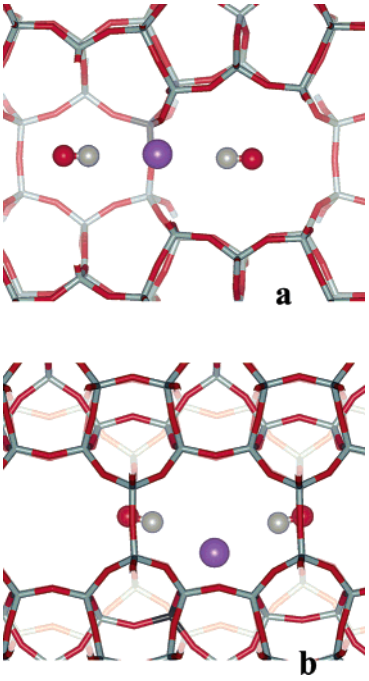

Figure 2. Dicarbonyl complexes formed on K^+ sites. (a) CO molecules on K^+ at I2/T2 site (view along the M channel) form almost perfectly linear OC−K−CO adduct, one molecule is located inside the P-cage (left) and the other one is located in the M channel (right). (b) Both CO molecules on M7/T3 site are located in the M channel (view along P channel). Framework O, Si, and Al atoms are depicted in red, gray, and black, respectively, using a tube mode. The K^+ ion and C and O atoms of CO are depicted as balls (violet, gray, and red, respectively).

K^+ site where formation of dicarbonyl species is not likely is P8/T1. At this site, the interaction energy with the second CO molecule is only about −5 kJ/mol.

Stability and CO frequencies were also investigated for O-down complexes (isocarbonyls). The O-down complex can be formed on each of the investigated K^+ sites with ΔE^{el} in the range −9.1 to −11.7 kJ/mol (Table 2). For the I2/T2, M7/T3, and I2/T4 sites the C−O stretching frequencies of O-down complexes are in the narrow range 2115−2117 cm^{-1}, while for P8/T1 site the value of $\nu_{CO} = 2107$ cm^{-1} was found.

3.1.3. CO Interaction with Dual K^+ Sites. Calculations for $K_4Al_4Si_{32}O_{72}$ unit cell were carried out with four CO molecules present in the FER channel system. Several configurations of framework Al and K^+ sites were considered. Two new types of complexes were identified (Figure 3).

(i) Linear K^+...CO...K^+ Complex. Here, CO is between two K^+ ions, having the C atom interacting with one K^+ ion and the O atom interacting with the other K^+ ion (Figure 3a). These complexes always show lower CO stretching frequency (ν_{CO} = 2141−2157 cm^{-1}, details below) and larger interaction energy (by about 5 kJ/mol) than complexes formed on isolated K^+ sites.

(ii) T-Shaped Complex. Here, CO interacts with one K^+ ion via the C-end, and both C and O atoms interact with the second K^+ ion in a T-shaped arrangement (Figure 3b). However, the stability of these complexes is lower than for complexes on isolated K^+ sites. Therefore, T-shaped complexes are not further discussed in this text.

For selected linearly bridged complexes, the calculations were carried out with $K_4Al_4Si_{32}O_{72}$ unit cell and only a single CO molecule present in the system. Structural parameters, interaction energies, and CO frequencies are reported in Table 3. Linear bridged K^+...CO...K^+ complexes are more stable (2−5 kJ/mol) than monocarbonyls. Depending on the K−K distance, the

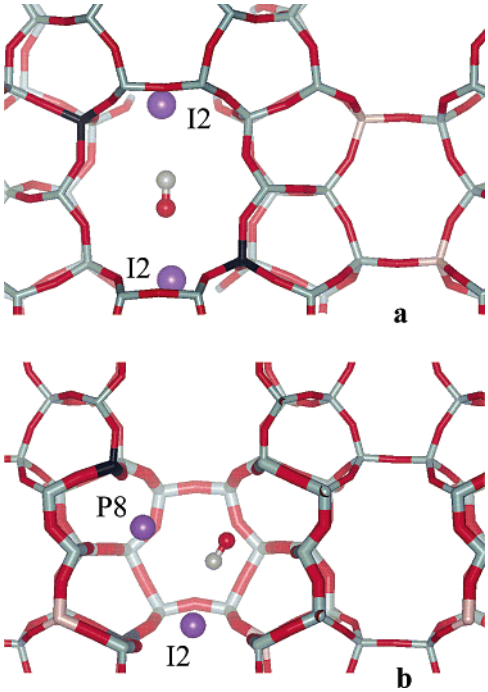

Figure 3. CO complexes on K^+ dual sites. (a) Bridged CO complex across the M channel, between two K^+ ions at I2/*T*4 sites. (b) T-shaped CO complex in P-cage, formed on K^+ ions at I2/T4 and P8/T1 sites. For coloring scheme, see caption for Figure 2.

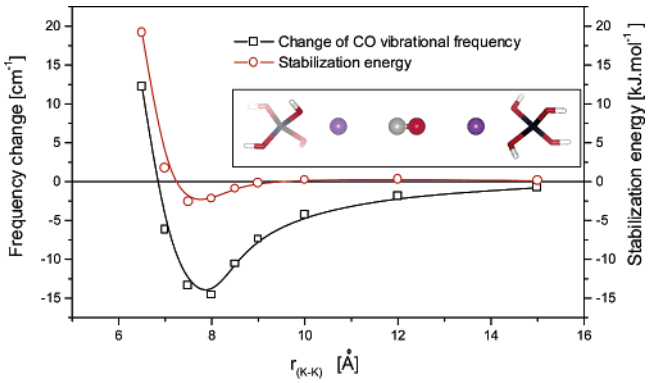

Figure 4. Dependence of stabilization energy due to the second K^+ ion (eq 2) and $\Delta\nu_{CO}$ on r(K−K) distance, calculated with 2x(1-T) cluster model (inset).

oxygen atom of CO may be closer to K^+ than the carbon atom. In fact, this is always the case for CO between a pair of K^+ ions in I2 sites (Table 3). The C−O stretching frequencies of bridged CO complexes were calculated using eq 1 for both C-down and O-down complexes, giving ν_{CO} values in the ranges 2154−2157 and 2141−2145, respectively. In fact, neither ω_{CO}/r_{CO} correlation for C-down nor for O-down adducts is ideal for the description of bridged species, where the electron density on CO is strongly affected on both ends. However, the experimentally determined C−O stretching frequency should be expected to fall between the limiting values calculated with correlation for C-down and O-down complexes. It should be pointed out that frequencies calculated with ω_{CO}/r_{CO} correlation method are still far better than those obtained in a standard way, even for the bridged CO complex.

To gain more understanding of linear K^+...CO...K^+ complexes, calculations with model 2x(1-T) cluster (Figure 4 inset) were performed. The dependence of the C−O stretching frequency shift, and the dependence of an additional stabilization interaction due to the dual K^+ site, on the separation between

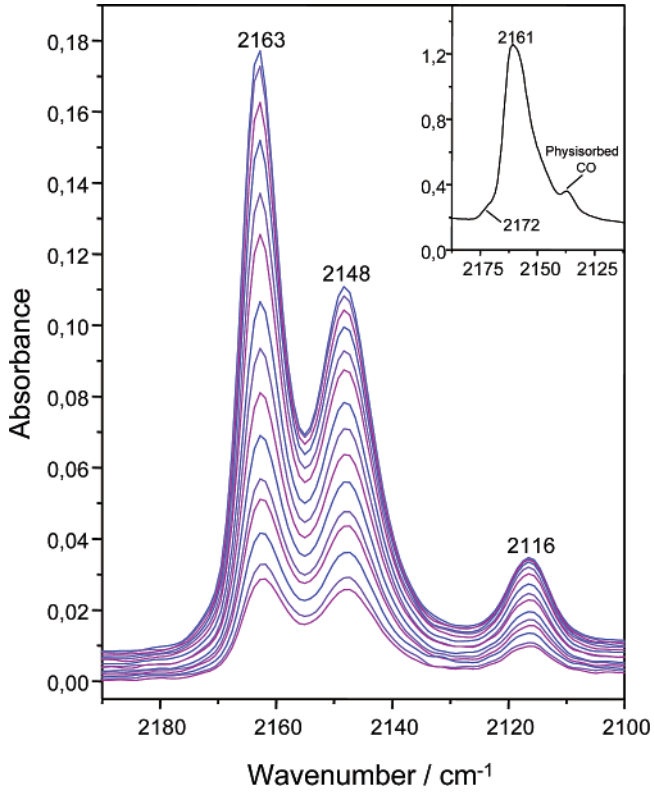

Figure 5. Variable-temperature FTIR spectra (zeolite blank subtracted) of CO adsorbed on K-FER, Si:Al = 27.5:1. From top to bottom, temperature goes from 176 to 223 K; and pressure from 0.12 to 0.64 Torr. Inset shows the spectrum obtained at 77 K for a larger dose of CO (about 2 Torr).

two K^+ ions is depicted in Figure 4. The additional stabilization interaction on the dual site is defined as

$$\Delta E^{el}(\text{dual}) = [E^{el}(\text{2x1-T...CO}) - E^{el}(\text{2x1-T}) - E^{el}(\text{CO})] - [E^{el}(\text{1-T...CO}) - E^{el}(\text{1-T}) - E^{el}(\text{CO})] \quad (2)$$

where the terms in first and second square brackets represent the CO interaction with dual and single site, respectively (interaction energies include BSSE correction). The frequency change due to the second cation was calculated as a difference between the frequency on isolated and dual site, both of them obtained from the ω_{CO}/r_{CO} correlation. The largest stabilization due to the presence of the second K^+ cation was found for an r(K−K) separation of about 7.5 Å. The largest red-shift of CO-stretching frequency (about 15 cm^{-1}) was found for r(K−K) separation in the range 7.5−8.0 Å.

3.2. Variable-Temperature FTIR Spectroscopy. *3.2.1. Spectroscopic Features and Adsorption Enthalpy.* Variable-temperature FTIR spectra (in the CO stretching region) of CO adsorbed on K-FER are shown in Figure 5. Main IR absorption bands are seen at 2163, 2148, and 2116 cm^{-1}. In addition, a weak shoulder, at about 2172 cm^{-1}, is clearly revealed at a relatively high CO dose (inset in Figure 5). The 2163 cm^{-1} band is assigned to CO interacting only through the C atom with a K^+ ion, while the 2148 cm^{-1} band should correspond to CO molecules bridging two K^+ cations. The 2116 cm^{-1} band corresponds to the O-down CO counterpart of the band at 2163 cm^{-1}.

A set of IR spectra recorded over a temperature range, while simultaneously measuring temperature and CO equilibrium pressure, can be used to determine the standard adsorption enthalpy ΔH^0 by using the VTIR method described in detail

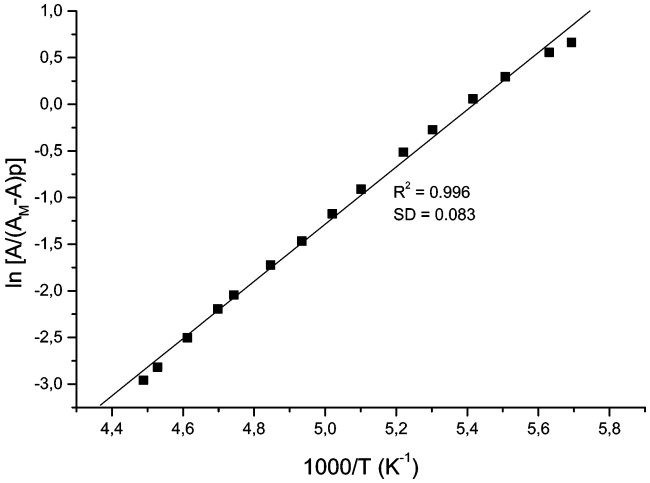

Figure 6. Plot of the left-hand side of eq 5 against reciprocal temperature for the band at 2163 cm^{-1} in Figure 5. R, linear regression coefficient; and SD, standard deviation.

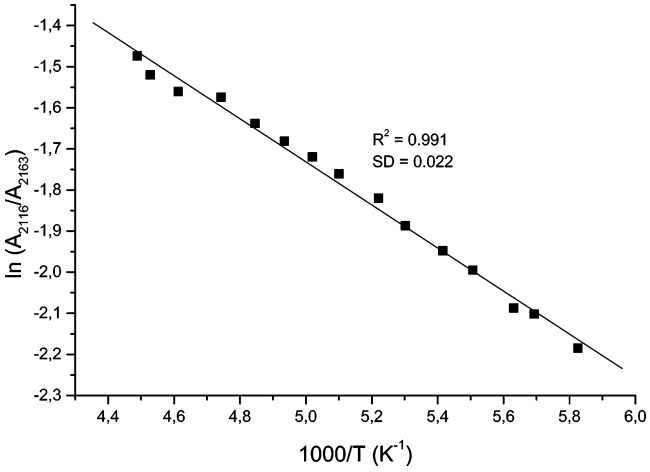

Figure 7. Plot of the natural logarithm of the intensity ratio of bands at 2116 (isocarbonyl) and 2163 cm^{-1} (carbonyl) versus reciprocal temperature.

elsewhere.[35] Briefly, at any given temperature, the integrated intensity of a characteristic IR absorption band should be proportional to the fractional coverage, θ, of the adsorbed species giving rise to such a band. Integrated band intensity, A, temperature, T, and CO equilibrium pressure, p, can be considered to be interrelated by the Langmuir type eq 3 below:

$$\theta = A/A_M = k(T)p/[1 + k(T)p] \quad (3)$$

where A_M stands for the integrated intensity corresponding to full coverage ($\theta = 1$) and k is the adsorption equilibrium constant. Equation 3 can be combined with the well-known van't Hoff eq 4, to yield eq 5 below:

$$\ln k = (-\Delta H^0/RT) + (\Delta S^0/R) \quad (4)$$

$$\ln(A/(A_M - A)p) = (-\Delta H^0/RT) + (\Delta S^0/R) \quad (5)$$

Equation 5 allows ΔH^0 and ΔS^0 to be determined from a set of IR spectra recorded over a temperature range.

After computer deconvolution of the variable-temperature IR spectra shown in Figure 5, and integration of the set of bands at 2163 cm^{-1}, the linear plot depicted in Figure 6 was obtained. Note that the needed value of A_M (for which only an approximate value was experimentally determined) was chosen as that giving the best linear fit of eq 5 for the whole set of experimental data (see ref 35 for details). The corresponding value resulted to be $A_M = 7.5$ cm^{-1}. From this A_M value, it was inferred that the experimental points in Figure 6 correspond to a coverage range of $0.05 < \theta < 0.25$. From the linear plot in Figure 6, the standard adsorption enthalpy was determined to be $\Delta H^0 = -25$ kJ/mol, and the corresponding entropy change (ΔS^0) is -138 J/(mol K). Taking into account possible errors due to both experimental measurements and band deconvolution, the estimated error limits are about ± 3 kJ/mol for enthalpy and ± 10 J/(mol K) for entropy.

The above procedure could not be applied for determining the standard adsorption enthalpy of the adsorbed CO species giving rise to the IR absorption band at 2148 cm^{-1} (Figure 5). The reason is that this band was experimentally observed to take a very long time to attain a constant intensity value, which made it impractical to obtain reliable quantitative intensity measurements (see section 4).

3.2.2. Isomerization Equilibrium between the K^+CO and K^+OC Species. Previous FTIR studies on CO adsorption on the MFI-type zeolites Na-ZSM-5 and K-ZSM-5 have shown[4,36] that the carbonyl (M^+CO) and isocarbonyl (M^+OC) species, where M^+ stands for the alkali-metal cation, are in a temperature-dependent isomerization equilibrium. For K-FER, such an equilibrium can be described by eq 6 below, where Z stands for zeolite framework:

$$Z^-K^+\cdots CO \rightleftarrows Z^-K^+\cdots OC \quad (6)$$

The equilibrium constant, k, of eq 6 should be equal to the ratio θ_{OC}/θ_{CO}, where θ_{OC} and θ_{CO} are the fractional coverages of isocarbonyl and carbonyl species, respectively. Hence, if A_{2163} and A_{2116} are the integrated absorbances of the corresponding IR bands, and ϵ_{2163} and ϵ_{2116} are (respectively) the molar absorption coefficients of K^+CO and K^+OC species, we have

$$k = (A_{2116}/A_{2163})(\epsilon_{2163}/\epsilon_{2116}) \quad (7)$$

The temperature dependence of k is given by the van't Hoff eq 4 above, which combined with eq 7 yields

$$\ln(A_{2116}/A_{2163}) = (-\Delta H^0/RT) + (\Delta S^0/R) + \ln(\epsilon_{2116}/\epsilon_{2163}) \quad (8)$$

From eq 8, the isomerization enthalpy can be derived. Note that knowledge of molar absorption coefficients is not needed.

Values of A_{2163} for spectra taken over a range of temperature were determined as stated in section 3.2.1. For the band at 2116 cm^{-1}, it should be noted that the ^{13}CO counterpart of the 2163 cm^{-1} band occurs in the same frequency region. For this reason, integrated A_{2116} values were corrected by subtracting 1% of the corresponding A_{2163} values; 1% is approximately the natural abundance of the ^{13}C isotope.

Figure 7 shows the plot of $\ln(A_{2116}/A_{2163})$ as a function of reciprocal temperature. From this linear plot, the value of $\Delta H^0 = 4.0$ kJ/mol was deduced for the isomerization equilibrium described by eq 6. The overall error limit was estimated to be ± 1 kJ/mol. Within this limit, the enthalpy change in the isomerization process described by eq 6 is about the same as that of $\Delta H^0 = 3.2$ kJ/mol reported[36] for the thermal isomerization equilibrium between K^+CO and K^+OC species formed upon CO adsorption on the zeolite K-ZSM-5.

4. Discussion

Experimental IR spectra (Figure 5) showed that CO adsorbed on K-FER gives rise to three main absorption bands, at 2163,

2148, and 2116 cm^{-1}, and a weak band (shoulder) at about 2172 cm^{-1}. Periodic DFT calculations showed that the CO molecule can bind to K^+ ions forming (i) monodentate monocarbonyls, (ii) monodentate dicarbonyls, and (iii) CO linearly bridging two nearby K^+ cations (dual cation sites). Calculated C−O stretching frequencies match very well with those of experimentally observed IR bands. Therefore, these bands can be confidently assigned as follows: (i) The dominant IR absorption band at 2163 cm^{-1} corresponds to C-down monodentate complexes (monocarbonyls) in which the CO molecule interacts with K^+ only through the carbon atom. (ii) The shoulder at 2172 cm^{-1} corresponds also to C-down monodentate CO complexes (monocarbonyls) on a K^+ ion. However, this band can be observed only for K^+ located in the P channel cavity (P8/T1 site). (iii) The 2116 cm^{-1} band comes from isocarbonyl species, where the CO molecule binds through the oxygen atom to a K^+ ion. This isocarbonyl band is the counterpart of that at 2163 cm^{-1} (carbonyl). (iv) The 2148 cm^{-1} band has to be assigned to the bridged CO complexes.

From calculations, it appears that the K^+ sites giving rise to monodentate carbonyls split into two groups distinguishable in IR spectra of adsorbed CO molecules. First, the carbonyl complexes formed on K^+ ions in I2 and M7 sites give rise to the IR band at 2163 cm^{-1}, and both mono- and dicarbonyl C-down species can be formed on these sites. Second, the carbonyl complexes on K^+ at P8 sites correspond to the shoulder at 2172 cm^{-1}; only monocarbonyl species can be formed at these sites. It should be noted that low intensity of 2172 cm^{-1} shoulder corresponds to, first, slightly lower stability of monocarbonyl complex at P8 site as compared to other sites, and, second, low population of T1 sites (T1:T2:T3:T4 = 1:2:2:4). An O-down complex can also be formed at P8 sites, having a C−O stretching frequency of 2106 cm^{-1}; however, due to the low population of these sites and to a lower stability of the O-down (as compared to the C-down) adduct, this feature is not observed experimentally.

The P8 sites are located in the P-channel cavity while I2 and M7 sites are at channel intersections and in the M channel, respectively (Figure 1). In addition to the results obtained for the P8/T1 site (reported in Table 2), CO interaction with the K^+ ion at P8/T3 and P8/T4 sites was also investigated. While these sites are higher in energy, and therefore less likely to be populated, the CO stretching frequency of C-down monodentate complexes formed on these sites appears also at 2172 cm^{-1}. We conclude that location of the cation in K-FER has the major impact on the C−O stretching frequency of monodentate complexes. Due to the relatively large size of the K^+ ion and the limited space available in the P channel cavity, CO interaction with the channel wall (leading to an additional blue-shift of the CO stretching frequency[24]) is more pronounced for P8 sites than for intersection and main channel sites (I2 and M7).

To our knowledge, this is the first time that evidence is put forward that cation location within the zeolite channel system has a significant effect on the stretching frequency of the adsorbed molecule. This effect is directly related to the size of the cation. For a small cation, like Li^+, it was shown that the CO stretching frequencies depend primarily on Li^+ coordination to the framework.[15,29,37] On the contrary, the results reported here show that K^+ coordination to the framework does not play a major role in determining the stretching frequency of adsorbed CO. The K^+ ion has different coordination (to framework oxygens) in M7 and I2 sites (4 and 5, respectively), and yet the CO stretching frequency is the same for both sites.

Concerning dicarbonyl species, calculations show that they can be formed on several K^+ sites (I2 and M7). They are characterized by bond lengths just marginally larger than those of isolated carbonyls and are, consequently, by frequencies only about 3 cm^{-1} smaller. Similarly, the enthalpy of formation of the dicarbonyl species is systematically smaller than that of the monocarbonyl, although by an amount only of the order of 1 kJ/mol (1.5 and 0.6 kJ/mol for I2 and M7 sites, respectively). Although these differences might appear to be negligible, they do find a direct correspondence in the experimental results. Figure 5 (inset) shows that when CO equilibrium pressure is increased the monocarbonyl band at 2163 cm^{-1} shifts to 2161 cm^{-1} (due to increased formation of dicarbonyls), in excellent agreement with the calculated values. However, for a coverage within the range $0.05 < \theta < 0.25$ (spectra in the main body of Figure 5), monocarbonyls are by far the dominant species, and the IR absorption band stays at 2163 cm^{-1}.

It remains to discuss the band at 2148 cm^{-1} (Figure 5). A similar IR absorption band was reported in the literature for CO adsorbed on K−FER, Na-MOR, and some other alkali-metal-exchanged zeolites,[5,6,36] and it was suggested by several authors that such a band can be due to multiple interaction of the adsorbed CO molecule with cations.[5,6] However, no detailed analysis was reported so far. The results of periodic DFT calculations given in Table 3 clearly show that the 2148 cm^{-1} IR absorption band arises from the CO molecule interacting simultaneously (through the carbon and the oxygen atom, Figure 3a) with two K^+ ions. The calculated CO stretching frequency for the linearly bridged complex thus formed falls within the limits of 2141 and 2157 cm^{-1} (depending on the model used for frequency calculation, see section 3.1.1). The experimentally observed value of 2148 cm^{-1} is just in the middle of this frequency range, which is strong evidence that this band really corresponds to the CO molecule interacting through both ends with two nearby K^+ cations (dual cation sites). This interpretation is in accordance with the results of the 2x(1-T) model (Figure 4) which show that, first, CO interaction with the second K^+ ion results in additional energy stabilization of such a carbonyl complex and, second, the C−O vibration frequency is significantly lowered (as compared to that of regular monocarbonyls). Frequency is increased by the polarization on the C-end and decreased by the polarization on the O-end, resulting in a C−O stretching frequency relatively close to the gas-phase value (2143 cm^{-1}). Note that this situation is quite different from that known to occur for bridging carbonyl ligands in many polynuclear transition metal ion complexes, where the bridging ligand binds to two transition metal ions through the carbon atom.

Since dual cation sites capable of bridging CO should be more abundant in K-FER having a lower Si/Al ratio, the band at 2148 cm^{-1} should be more prominent for such a case. As a further test, Figure 8 shows spectra of CO adsorbed, at about the same CO equilibrium pressure, on K-FER samples with Si/Al = 27.5 and Si/Al = 8.6. It is clearly seen that the 2148 cm^{-1} band becomes dominant in the case of the lower-silica sample, thus providing strong additional evidence that this band corresponds to the bridged CO species.

For a better understanding of the CO complexes in K-FER, it is useful to consider the distribution of the K^+ cations among the different sites in the zeolite. Figure 9 shows a sketch of the FER channel structure, and location of K^+ ions and CO complexes in K-FER for the both high-silica (part a) and low-silica (part b) cases. In the high-silica case, monocarbonyl complexes can be formed on K^+ ions at I2 (both I2/T2 and

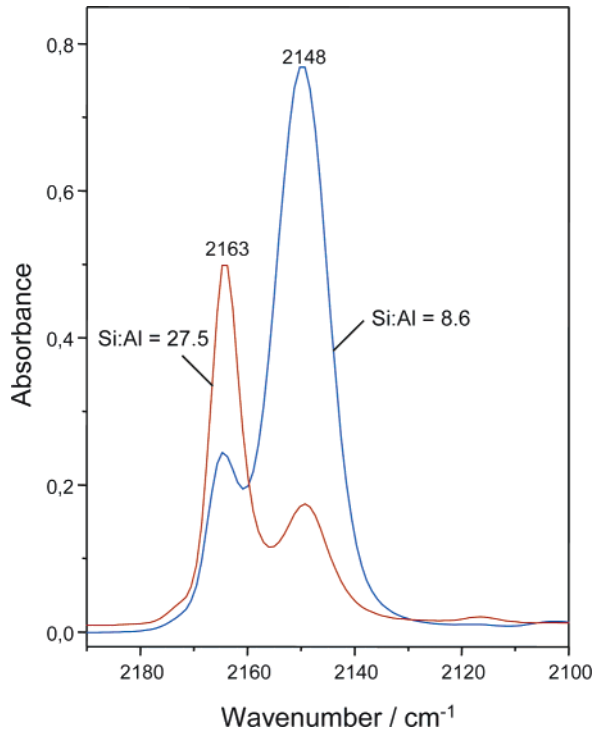

Figure 8. IR spectra of CO adsorbed, at 77 K and about 0.06 Torr (equilibrium pressure), on K-FER samples having different Si:Al ratios, 27.5 and 8.6, respectively.

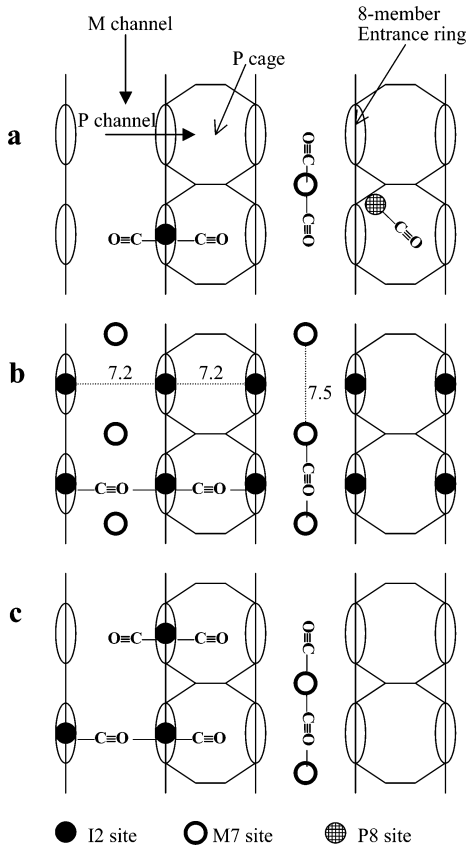

Figure 9. Sketch of possible CO adsorption complexes in K-FER for high-silica, low-silica, and intermediate Si/Al ratio cases (parts a, b, and c, respectively). The main and perpendicular channels run along vertical and horizontal directions, respectively; eight-member ring entrance window of P-cage is depicted as an oval. Intersection I2 sites (located inside the eight-member ring window), main channel M7 sites, and P-cage P8 sites are depicted as filled, empty, and textured circles, respectively. (a) High-silica system, where isolated K^+ sites prevail, forming monodentate mono- and dicarbonyl. (b) Low-silica system, where large K^+ loading results in occupation of nearly all I2 and M7 sites; thus, dual K^+ sites prevail and bridged CO complexes are formed. (c) Intermediate Si/Al ratio. Both isolated and dual K^+ sites exist, and both monodentate and bridged complexes can be formed.

I2/T4), M7 (M7/T3), and P8 (P8/T1) sites, and in addition, dicarbonyl complexes can also be formed on I2 and M7 sites. In the case of low-silica FER, a high K^+ concentration results in a dense population of I2 and M7 sites. This highly favors appearance of pairs of K^+ ions (dual sites) about 7.2−7.5 Å apart. This is the optimum distance for formation of linearly bridged CO complexes, as inferred from Figure 4. Hence, formation of bridged CO complexes in K-FER should be expected. Such bridged species can be readily formed between two K^+ ions in I2 sites (either across the M channel or across the P channel cavity) and also between two K^+ ions in neighboring M7 sites (along the main channel), as sketched in Figure 9b. For K-FER having an intermediate Si/Al ratio, both types of CO complexes (monodentate and bridged) can be formed. Note also that the same K^+ ion can participate in formation of bridged and monodentate CO complexes at the same time (Figure 9c).

Dual cation sites capable of forming a bridged CO complex are likely to be present not only in K-FER but also in other alkali-metal-exchanged zeolites as well. In fact, reported IR spectra[36] of CO adsorbed on K-ZSM-5 show main absorption bands at 2166 and 2150 cm^{-1}. In light of the above discussion, it becomes clear that the band at 2150 cm^{-1} corresponds to the bridged CO complexes. Similarly, CO adsorbed on Na-FER (Si/Al = 8) was shown[6] to give main IR adsorption bands at 2175 and 2159 cm^{-1}, and the latter band should correspond to the bridged CO species. Other examples for both K- and Na-zeolites can be found in the literature.

Let us now consider the adsorption enthalpy of CO on K-FER. For the species giving rise to the band at 2163 cm^{-1} (monocarbonyls) theoretical calculations give $\Delta H^0(200)$ values in the range −18.1 to −20.4 kJ/mol (Table 2), to be compared with the experimentally determined value of −25(±3) kJ/mol. A small discrepancy between the calculated and experimental enthalpies is most likely due to the fact that CO interaction with the zeolite channel wall has a nonnegligible contribution from dispersion forces. Note that for Silicalite-I the CO net differential adsorption enthalpy was reported to be −10 kJ/mol.[38] The DFT calculations performed in this study do not account for dispersion interactions; thus, it is not surprising that the calculated enthalpies are smaller than the experimental ones. However, the neglected dispersion interactions should be rather similar for all CO complexes investigated. Therefore, the relative interaction energies for individual complexes reported in Tables 2 and 3 are likely to be correct. For isomerization between carbonyls and isocarbonyls, the calculated $\Delta H^0(200)$ value is 4.2−5.3 kJ/mol, in very good agreement with the experimentally determined value of 4(±1) kJ/mol.

For the CO complex giving rise to the band at 2148 cm^{-1}, no corresponding band for any isomeric (O-down) species was observed. This is consistent with the assignment of the 2148 cm^{-1} band to a bridged CO species. Calculations show that the adsorption enthalpy of the bridged CO complexes is about 5 kJ/mol larger than that for monodentate species. As already said in section 3.2.1, no experimental value for the adsorption enthalpy of the bridged CO species could be determined, due to the fact that equilibrium could not be attained at low temperature. The reason for this might be that some of the dual sites could be blocked by the K^+ ion. In particular, the dual

site inside the P channel cage is hindered by the K^+ ions at I2 sites in the entrance windows of this cage (Figure 9). Therefore, the diffusion of CO in and out of these cages is likely to be very slow at a low temperature.

Finally, a comment on correlation between the C−O stretching frequency of adsorbed CO and interaction energy with the corresponding adsorption site seems to be pertinent. A direct correlation (i.e., higher stretching frequency for higher interaction energy) is often invoked in the literature concerning CO interaction with non-d, or d^{10}, cations.[39,40] However, results presented in Table 2 show that stability of the CO complex (monocarbonyl) on site P8 is lower than on site I2, while the C−O stretching frequency is higher on P8 than on I2. In addition, the bridged CO complex is about 5 kJ/mol more stable than the monodentate carbonyl, whereas the C−O stretching frequency is considerably smaller for the bridged complex. For the latter case, absence of correlation (between stretching frequency and interaction energy) is due to formation of an entirely new type of adsorption complex, i.e., the bridged CO species. In the former case, lack of correlation stems from additional interaction of adsorbed CO with the zeolite framework, which results in a blue-shift of the C−O stretching frequency.[24] Whichever the case, however, it should be clear that straightforward use of any direct correlation between frequency and interaction energy may be misleading.

5. Conclusions

The main conclusions can be summarized as follows. (i) Carbon monoxide adsorbed (at a low temperature and pressure) on K-FER forms two main types of adsorption complexes: monocarbonyls, where CO interacts via C atom with a single K^+ ion, and bridged CO complexes, where the CO molecule bridges two nearby K^+ ions (interacting through the C atom with one of them and through the O atom with the other one). To our knowledge, detailed analysis of the bridged CO complex is reported here for the first time. Both theoretical calculations (at the periodic DFT level) and IR spectroscopic data show that such bridged complexes can be expected to form not only in K-FER, but also on other alkali-metal-exchanged zeolites. The necessary condition is that two alkali-metal ions happen to be at the right distance apart from each other; about 7.5 Å in the case of K^+. Such a pair of metal ions, which can be bridged by adsorbed CO, constitutes a dual cation site. (ii) The C−O stretching frequency of monocarbonyl species in K-FER depends on K^+ location in the zeolite, and not on K^+ coordination to the framework. Combination of theoretical calculations and experimental results showed formation of two types of monocarbonyls. The most abundant type appears at 2163 cm^{-1}, and the less abundant one at 2172 cm^{-1}. These experimentally determined wavenumbers coincide, within ± 2 cm^{-1}, with those derived from theoretical calculations. (iii) For the monocarbonyl species giving rise to the IR absorption band at 2163 cm^{-1}, a CO standard adsorption enthalpy of $\Delta H^0 = -25(\pm 3)$ kJ/mol was derived from variable-temperature FTIR spectroscopy. The corresponding calculated value is of about −20 kJ/mol. Also noteworthy is that the calculated value of interaction energy for the bridged CO complex is about 5 kJ/mol larger than that of the monocarbonyl, despite the C−O stretching frequency being smaller (by about 15 cm^{-1}) in the bridged CO species. (iv) Finally, the whole set of results discussed shows that, by combining spectroscopic measurements with appropriate calculations on a periodic density functional model, detailed interpretation of IR spectra can be attained at the atomic scale level. When an appropriate model (respecting the details of zeolite topology) is used, the C−O stretching frequency of CO adsorbed on different site types can be calculated with nearly spectroscopic accuracy.

Acknowledgment. Work in Prague was supported by Grants of ME CR No. LC512, GA CR No. 203/06/0324, and project Z4 055 0506. The Spanish MEC and FEDER funds are gratefully acknowledged for supporting work done at the UIB (Project number: MAT2005-05350). Work in Pardubice was supported by Grants of ME CR No. 0021627501.

References and Notes

(1) Zecchina, A.; Arean, C. O. *Chem. Soc. Rev.* **1996**, *25*, 187.
(2) Knozinger, H.; Huber, S. *J. Chem. Soc., Faraday Trans.* **1998**, *94*, 2047.
(3) Hadjiivanov, K. I.; Vayssilov, G. N. *Adv. Catal.* **2002**, *47*, 307.
(4) Arean, C. O.; Tsyganenko, A. A.; Platero, E. E.; Garrone, E.; Zecchina, A. *Angew. Chem., Int. Ed.* **1998**, *37*, 3161.
(5) Montanari, T.; Kozyra, P.; Salla, I.; Datka, J.; Salagre, P.; Busca, G. *J. Mater. Chem.* **2006**, *16*, 995.
(6) Bordiga, S.; Turnes Palomino, G.; Paze, C.; Zecchina, A. *Microporous Mesoporous Mater.* **2000**, *34*, 67.
(7) Nachtigall, P. *Stud. Surf. Sci. Catal.* **2005**, *157*, 243.
(8) Tsyganenko, A. A.; Storozhev, P. Y.; Arean, C. O. *Kinet. Catal.* **2004**, *45*, 530.
(9) Arean, C. O.; Manoilova, O. V.; Tsyganenko, A. A.; Palomino, G. T.; Mentruit, M. P.; Geobaldo, F.; Garrone, E. *Eur. J. Inorg. Chem.* **2001**, 1739.
(10) Bludsky, O.; Silhan, M.; Nachtigall, P.; Bucko, T.; Benco, L.; Hafner, J. *J. Phys. Chem. B* **2005**, *109*, 9631.
(11) Vaughan, P. A. *Acta Crystallogr.* **1966**, *21*, 983.
(12) It should be pointed out that this numbering scheme differs from that used in Database of Zeolite Structures: http://www.iza-structure.org/databases/, where T1 and T4 positions are switched.
(13) Nachtigallova, D.; Nachtigall, P.; Sierka, M.; Sauer, J. *Phys. Chem. Chem. Phys.* **1999**, *1*, 2019.
(14) Arean, C. O.; Palomino, G. T.; Garrone, E.; Nachtigallova, D.; Nachtigall, P. *J. Phys. Chem. B* **2006**, *110*, 395.
(15) Nachtigall, P.; Bulanek, R. *Appl. Catal., A* **2006**, *307*, 118.
(16) Perdew, J. P.; Burke, K.; Ernzerhof, M. *Phys. Rev. Lett.* **1996**, *77*, 3865.
(17) Perdew, J. P.; Burke, K.; Ernzerhof, M. *Phys. Rev. Lett.* **1997**, *78*, 1396.
(18) Blochl, P. E. *Phys. Rev. B* **1994**, *50*, 17953.
(19) Kresse, G.; Joubert, D. *Phys. Rev. B* **1999**, *59*, 1758.
(20) Kresse, G.; Hafner, J. *Phys. Rev. B* **1993**, *48*, 13115.
(21) Kresse, G.; Hafner, J. *Phys. Rev. B* **1994**, *49*, 14251.
(22) Kresse, G.; Furthmuller, J. *Phys. Rev. B* **1996**, *54*, 11169.
(23) Kresse, G.; Furthmuller, J. *Comput. Mater. Sci.* **1996**, *6*, 15.
(24) Bludsky, O.; Silhan, M.; Nachtigallova, D.; Nachtigall, P. *J. Phys. Chem. A* **2003**, *107*, 10381.
(25) Bludsky, O.; Silhan, M.; Nachtigall, P. *J. Chem. Phys.* **2002**, *117*, 9298.
(26) Dunning, T. H. *J. Chem. Phys.* **1989**, *90*, 1007.
(27) Woon, D. E.; Dunning, T. H. *J. Chem. Phys.* **1993**, *98*, 1358.
(28) Iron, M. A.; Oren, M.; Martin, J. M. L. *Mol. Phys.* **2003**, *101*, 1345.
(29) Nachtigallova, D.; Nachtigall, P.; Bludsky, O. *Phys. Chem. Chem. Phys.* **2004**, *6*, 5580.
(30) Dolg, M. *Theor. Chim. Acta* **1996**, *93*, 141.
(31) Sadlej, A. J.; Urban, M. *THEOCHEM* **1991**, *80*, 147.
(32) Schafer, A.; Horn, H.; Ahlrichs, R. *J. Chem. Phys.* **1992**, *97*, 2571.
(33) Boys, S. F.; Bernardi, F. *Mol. Phys.* **1970**, *19*, 553.
(34) Frisch, M. J. et al., Gaussian 03; Gaussian Inc.: Pittsburgh, PA, 2003.
(35) Garrone, E.; Arean, C. O. *Chem. Soc. Rev.* **2005**, *34*, 846.
(36) Manoilova, O. V.; Mentruit, M. P.; Palomino, G. T.; Tsyganenko, A. A.; Arean, C. O. *Vib. Spectrosc.* **2001**, *26*, 107.
(37) Arean, C. O.; Delgado, M. R.; Manoilova, O. V.; Palomino, G. T.; Tsyganenko, A. A.; Garrone, E. *Chem. Phys. Lett.* **2002**, *362*, 109.
(38) Llewellyn, P. L.; Coulomb, J. P.; Grillet, Y.; Patarin, J.; Andre, G.; Rouquerol, J. *Langmuir* **1993**, *9*, 1852.
(39) Bolis, V.; Magnacca, G.; Morterra, C. *Res. Chem. Intermed.* **1999**, *25*, 25.
(40) Bolis, V.; Barbaglia, A.; Bordiga, S.; Lamberti, C.; Zecchina, A. *J. Phys. Chem. B* **2004**, *108*, 9970.